

## Averting cracks caused by insertion reaction in lithium-ion batteries

Yuhang Hu, Xuanhe Zhao, and Zhigang Suo<sup>a)</sup>

School of Engineering and Applied Sciences, Harvard University, Cambridge, Massachusetts 02138

(Received 1 February 2010; accepted 16 March 2010)

In a lithium-ion battery, both electrodes are atomic frameworks that host mobile lithium ions. When the battery is being charged or discharged, lithium ions diffuse from one electrode to the other. Such an insertion reaction deforms the electrodes and may cause the electrodes to crack. This paper uses fracture mechanics to determine the critical conditions to avert insertion-induced cracking. The method is applied to cracks induced by the mismatch between phases in  $\text{LiFePO}_4$ .

Lithium-ion batteries of high energy densities have rapidly become the batteries of choice for portable electronics.<sup>1</sup> These batteries are being further developed as a key part for the technology of clean and secure energy.<sup>2-4</sup> Battery-powered cars will reduce pollution, promote renewable energy, and maintain individual mobility.

At the heart of a lithium-ion battery is a process that couples electrochemistry and mechanics. In the battery, two electrodes are separated by an electrolyte. Each electrode is an atomic framework that conducts both lithium ions and electrons, while the electrolyte conducts lithium ions but not electrons. When the battery is being charged or discharged, the two electrodes are connected by an electronic conductor. The difference in the electrochemical potentials of lithium in the two electrodes motivates lithium ions to move from one electrode to the other through the electrolyte. To maintain electrical neutrality, electrons flow from one electrode to the other through the electronic conductor. This process, in which an atomic framework absorbs or releases mobile atoms, is known as an insertion reaction.<sup>5,6</sup> When large amounts of lithium atoms are inserted into or extracted from the framework, the electrodes deform substantially.

The insertion-induced deformation is often constrained by the mismatch between active and inactive materials, between grains of different crystalline orientations, and between phases of different concentrations of lithium (Fig. 1). Under such constraints, the insertion or extraction of lithium induces in an electrode a field of stress, which may cause the electrode to form cracks.<sup>7-9</sup> The cracks may break pieces of active material from the electrode, causing the capacity of the battery to fade.<sup>9,10</sup> The cracks also expose fresh surfaces of active materials to the electrolyte, possibly degrading the chemical stability and safety of the battery.<sup>10</sup>

This paper describes a method to determine conditions that avert insertion-induced cracking. To focus on essential ideas, we consider cracks caused by the mismatch between different phases in  $\text{LiFePO}_4$ , a material used as cathodes because of its high energy density, low cost, and thermal stability.<sup>11</sup> Although  $\text{LiFePO}_4$  has low electronic conductivity in its native state, electrochemical performance can be improved substantially in many ways, such as carbon coating,<sup>12</sup> doping,<sup>13,14</sup> and reducing particle size.<sup>15,16</sup> Our calculation determines the critical size of particles, below which cracking will not occur. This conclusion is consistent with existing experimental observations.<sup>10,17,18</sup> Insertion-induced cracking in batteries have been analyzed in previous studies, using thin-film model<sup>19</sup> and core-shell model.<sup>20-23</sup> Here we describe a model on the basis of realistic geometry of  $\text{LiFePO}_4$  particles.

Our model is formulated in terms of fracture mechanics.<sup>24</sup> Cracklike flaws are assumed to pre-exist in a crystalline particle of  $\text{LiFePO}_4$ . The particle is in a state of stress caused by the mismatch between two phases of the crystal. We ask if the stress will cause any of the flaws to advance. The elastic energy in the particle reduces when a crack advances. The reduction of the elastic energy in the particle associated with the crack advancing a unit area defines the energy release rate  $G$ . Dimensional considerations dictate that the energy release rate should take the form

$$G = ZE\varepsilon_m^2 d \quad , \quad (1)$$

where  $E$  is an elastic modulus,  $\varepsilon_m$  a mismatch strain, and  $d$  a length characteristic of the size of the particle. The dimensionless coefficient  $Z$  is determined by solving the boundary-value problem of elasticity.

As the crack advances in the particle, the elastic energy of the particle reduces, but the area of the crack increases. The crack cannot advance if

$$G < 2\gamma \quad , \quad (2)$$

where  $\gamma$  is the surface energy.

<sup>a)</sup>Address all correspondence to this author.

e-mail: suo@seas.harvard.edu

DOI: 10.1557/JMR.2010.0142

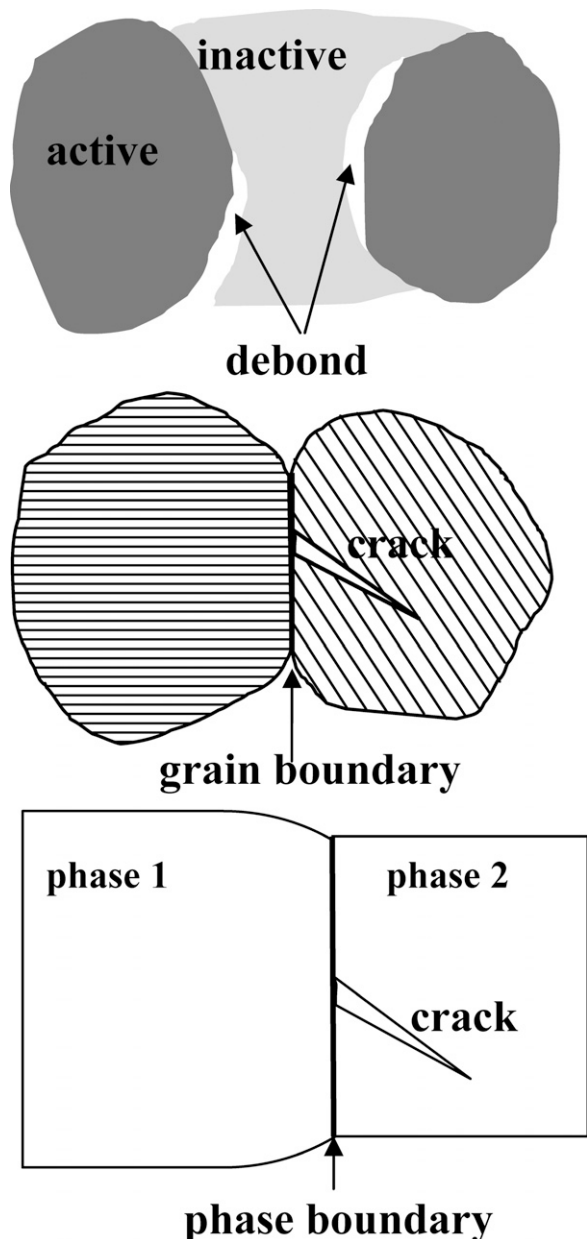


FIG. 1. Insertion-induced deformation may be constrained by the mismatch between active and inactive materials, between grains of different orientations, and between phases of different concentrations of lithium. The constrained deformation leads to stresses, which may cause the electrode to crack.

One difficulty in applying fracture mechanics is that the dimensionless coefficient  $Z$  varies with a large number of parameters, including ratios of various elastic moduli, of various mismatch strains, and of various lengths. To circumvent this difficulty, we adopt the following approach. We will study particles of shapes observed in experiments. Once the particle is given,  $Z$  can still vary with the location and length of the crack. We assume that the crack is on the cleavage planes of the crystal and then vary the length of the crack to maximize  $Z$ .

When all parameters are fixed except for the length of the crack,  $Z$  is a function of the dimensionless ratio:

$$Z = f\left(\frac{L}{d}\right) \quad , \quad (3)$$

where  $L$  is the length of the crack. Denote the maximal value of this function by  $Z_{\max}$ . No cracks can advance if the crack of maximal energy release rate is below the surface energy, namely,

$$Z_{\max} E \varepsilon_m^2 d < 2\gamma \quad . \quad (4)$$

This condition defines a critical particle size, given by

$$d_{\text{critical}} = \frac{2\gamma}{Z_{\max} E \varepsilon_m^2} \quad . \quad (5)$$

When the particle is smaller than this critical size, no pre-existing cracks in the particle can advance.

The aforementioned approach has been used to analyze many systems, such as polycrystals,<sup>25</sup> composites,<sup>26</sup> and thin films.<sup>27</sup> We now apply this approach to particles of  $\text{LiFePO}_4$ .  $\text{LiFePO}_4$  is an atomic framework of the olivine structure (Fig. 2). In the  $b$  direction of the framework are tunnels, in which lithium ions diffuse.<sup>9,17,18,28</sup> The crystal has two phases: the lithium-rich phase noted as  $\text{LiFePO}_4$ , and the lithium-poor phase noted as  $\text{FePO}_4$ . The lattice constants of the  $\text{LiFePO}_4$  phase are  $a = 10.33 \text{ \AA}$ ,  $b = 6.01 \text{ \AA}$ , and  $c = 4.69 \text{ \AA}$ , while the lattice constants of the  $\text{FePO}_4$  phase are  $a = 9.81 \text{ \AA}$ ,  $b = 5.79 \text{ \AA}$ , and  $c = 4.78 \text{ \AA}$ .<sup>23</sup> Consequently, upon absorbing lithium and changing phase, the crystal deforms by a state of triaxial strains:

$$\varepsilon_a = 5.03\%, \varepsilon_b = 3.7\%, \varepsilon_c = -1.9\% \quad . \quad (6)$$

This state of strains is anisotropic.

We analyzed the field of stress by using a commercial finite element package, ABAQUS. The mismatch strains associated with the phase transition, Eq. (6), were applied as if they were caused by thermal expansion. The particles were assumed to deform under no external constraint. The crack tip was densely meshed, with the smallest element around the crack tip being  $10^{-4}$  times

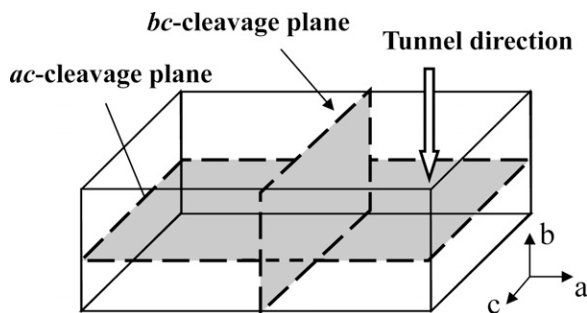


FIG. 2. In a crystal of  $\text{LiFePO}_4$ , lithium atoms diffuse along tunnels in direction  $b$ , and cleavage may occur on the  $bc$  and  $ac$  planes.

the crack length. The  $J$  integral was used to calculate the energy release rate. Orthotropic elastic constants used in this simulation were obtained by Maxisch and Ceder<sup>29</sup> using first-principle calculations. Following experimental observations,<sup>17</sup> we assumed that the particles were either platelike or equiaxed.

Figure 3 illustrates a platelike particle, where the phase boundary is the  $bc$  plane. We consider a crack on this plane. The observed average dimensions of the platelike particles were  $4 \times 2 \times 0.2 \mu\text{m}$ .<sup>17</sup> The thickness of the particles was much smaller than the lateral dimensions, so that the plates were taken to deform under the plane-stress conditions. The calculated energy release rate is plotted as a function of the crack length. When the crack is short, the elastic energy in the particle does not change appreciably when the length of the crack changes, and the energy release rate is small. When the crack is long, the elastic energy in the particle is nearly fully relaxed, and the energy release rate is also small. The energy release rate maximizes when the crack is of an intermediate length, giving  $Z_{\text{max}} = 0.0363$ . The surface energy of  $bc$  plane from the first-principles calculation is  $\gamma_{bc} = 0.66 \text{ J/m}^2$ .<sup>29</sup> The value of  $c_{11}$  in the stiffness matrix of  $\text{FePO}_4$  was used for normalization, which is 166.5 GPa. From Eq. (5), the critical size of the platelike particle is estimated to be  $d_{\text{critical}} = 605 \text{ nm}$ .

Figure 4 illustrates particles of an equiaxed shape. The equiaxed particles were taken to deform under the plane-strain conditions. Experimental observations have shown that the phase boundary is on the  $ac$  plane, and the crack can be on the two cleavage planes,  $bc$  plane, or  $ac$  plane.<sup>17</sup> In the finite-element calculation, the equiaxed particle is taken to deform under the plane strain conditions. Figure 4(a) plots the calculated energy release rate as a function of the crack length for a crack on the  $bc$  plane, giving  $Z_{\text{max}} = 0.0065$ . In this configuration, the  $\text{LiFePO}_4$  phase is under compression near the phase boundary, but is under tension near the face of the parti-

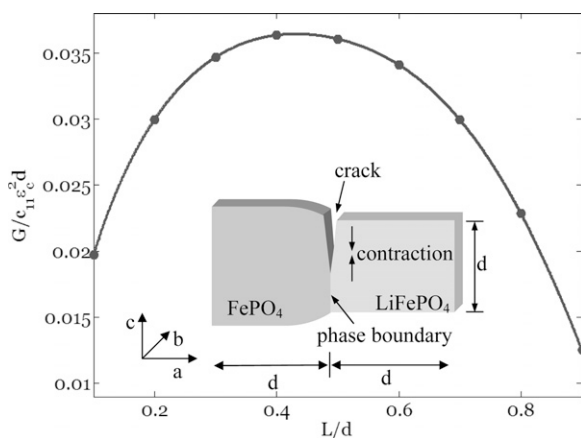


FIG. 3. Energy release rate for a crack on the phase boundary in a platelike  $\text{LiFePO}_4$  particle.

cle, where a crack is taken to initiate. Figure 4(b) plots the calculated results for a crack on the  $ac$  plane, giving  $Z_{\text{max}} = 0.0524$ . Consequently, the critical particle size should be determined by the crack on the  $ac$  plane. The crack is induced by elongation of  $\text{FePO}_4$  during insertion in  $a$  direction. Again based on first principle, the elastic modulus in  $a$  direction is 166.5 GPa and surface energy of  $ac$  plane  $\gamma_{ac} = 0.64 \text{ J/m}^2$ .<sup>29</sup> Similarly, the critical particle size for equiaxed particle calculated from Eq. (5) is  $d_{\text{critical}} = 58 \text{ nm}$ .

Experimental observations of cracked particles reported in the literature are limited. Cracks were found in a platelike particle of dimensions  $4 \times 2 \times 0.2 \mu\text{m}$ .<sup>17,18</sup> Cracks were also found in equiaxed particles of size 300 to 600 nm and 200 nm.<sup>9,17</sup> Also when particle size is smaller than 30 nm, no fracture was observed.<sup>30</sup> These experimental observations are consistent with the critical particle size calculated in this paper.

To further test the accuracy of this model, more experimental data on cracks in particles of different sizes and shapes are needed. In reality, the crack may initiate from sites other than those simulated in this paper. For example, for the equiaxed particle shown in Fig. 4(a), the  $\text{FePO}_4$  phase is under tension near the phase boundary,

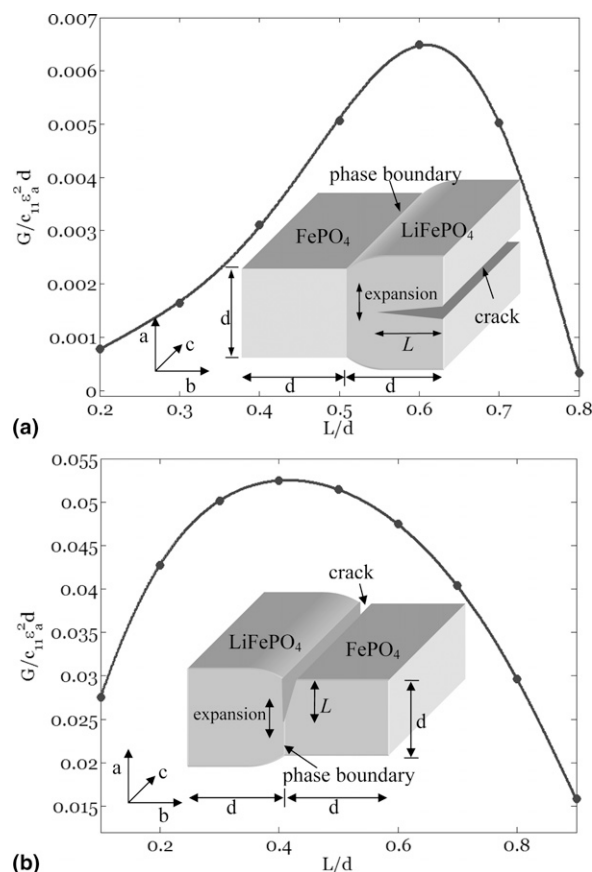


FIG. 4. In an equiaxed  $\text{LiFePO}_4$  particle, energy release rate of (a) a crack in a phase and (b) a crack on the phase boundary.

where the crack may initiate. We have not simulated all possible sites of crack imitation, but have illustrated the approach using configurations in Figs. 3 and 4. In addition, in calculating critical particle sizes, we have used the elastic moduli and surface energies determined by first-principles calculations.<sup>29</sup> It is well known that the critical energy release rate is typically larger than two times the surface energy.<sup>24</sup> Both the elastic moduli and critical energy release rates should be ascertained by future experiments.

In summary, we have applied fracture mechanics to study insertion-induced cracking in LiFePO<sub>4</sub> particles caused by the mismatch between different phases. We estimate the maximal energy release rate among various cracks. When the maximal energy release rate is below the critical value, no cracks in the particle can advance. This approach enables us to calculate the critical particle size to avert insertion-induced cracking. We hope that more experimental data will be made available to compare with the theoretical calculation.

## ACKNOWLEDGMENTS

The authors are grateful to the support by NSF through the MRSEC, and by the Kavli Institute at Harvard.

## REFERENCES

- G.A. Nazri and G. Pistoia: *Lithium Batteries: Science and Technology* (Kluwer Academic Publishers, Boston, MA, 2003).
- Basic Research Needs to Assure a Secure Energy Future (U.S. Department of Energy, Washington, DC, 2003).
- Basic Research Needs for Electrical Energy Storage (U.S. Department of Energy, Washington, DC, 2007).
- M. Broussely and G. Pistoia: *Industrial Applications of Batteries* (Elsevier, Amsterdam, 2007).
- P.G. Bruce: *Solid State Electrochemistry* (Cambridge University Press, 1995).
- R.A. Huggins: *Advanced Batteries* (Springer, New York, NY, 2009).
- J. Go and I. Pyun: Investigation of stresses generated during lithium transport through the RF sputter-deposited Li<sub>1-δ</sub>CoO<sub>2</sub> film by DQCR technique. *J. Electrochem. Soc.* **150**, A1037 (2003).
- Y. Ito and Y. Ukyo: Performance of LiNiCoO<sub>2</sub> materials for advanced lithium-ion batteries. *J. Power Sources* **146**, 39 (2005).
- D. Wang, X. Wu, Z. Wang, and L. Chen: Cracking causing cyclic instability of LiFePO<sub>4</sub> cathode material. *J. Power Sources* **140**, 125 (2005).
- K.E. Aifantis and S.A. Hackney: An ideal elasticity problem for Li-batteries. *J. Mech. Behav. Mater.* **14**, 413 (2003).
- K. Zaghib, J. Shim, A. Guerfi, P. Charest, and K. Striebel: Effect of carbon source as additives in LiFePO<sub>4</sub> as positive electrode for lithium-ion batteries. *Electrochem. Solid-State Lett.* **8**, A207 (2005).
- S.Y. Chung, J.T. Bloking, and Y.M. Chiang: Electronically conductive phosphor-olivines as lithium storage electrodes. *Nat. Mater.* **1**, 123 (2002).
- S.P. Herle, B. Ellis, N. Coombs, and L.F. Nazar: Nano-network electronic conduction in iron and nickel olivine phosphates. *Nat. Mater.* **3**, 147 (2004).
- F. Croce, A.D. Epifanio, J. Hassoun, A. Deptula, T. Olczac, and B. Scrosati: A novel concept for the synthesis of an improved LiFePO<sub>4</sub> lithium battery cathode. *Electrochem. Solid-State Lett.* **5**, A47 (2002).
- A. Yamada, S.C. Chung, and K. Hinokuma: Optimized LiFePO<sub>4</sub> for lithium battery cathodes. *J. Electrochem. Soc.* **148**, A224 (2001).
- C. Delacourt, P. Poizot, S. Levasseur, and C. Masquelier: Size effects on carbon-free LiFePO<sub>4</sub> powders. *Electrochem. Solid-State Lett.* **9**, A352 (2006).
- H. Gabrisch, J. Wilcox, and M.M. Doeff: TEM study of fracturing in spherical and plate-like LiFePO<sub>4</sub> particles. *Electrochem. Solid-State Lett.* **11**, A25 (2008).
- G. Chen, X. Song, and T.J. Richardson: Electron microscopy study of the LiFePO<sub>4</sub> to FePO<sub>4</sub> phase transition. *Electrochem. Solid-State Lett.* **9**, A295 (2006).
- R.A. Huggins and W.D. Nix: Decrepitation model for capacity loss during cycling of alloys in rechargeable electrochemical systems. *Ionics* **6**, 57 (2000).
- K.E. Aifantis, S.A. Hackney, and J.P. Dempsey: Design criteria for nanostructured Li-ion batteries. *J. Power Sources* **165**, 874 (2007).
- X.C. Zhang, W. Shyy, and A.M. Sastry: Numerical simulation of intercalation-induced stress in Li-ion battery electrode particles. *J. Electrochem. Soc.* **154**, A910 (2007).
- J. Christensen and J. Newman: Stress generation and fracture in lithium insertion materials. *J. Electrochem. Soc.* **153**, A1019 (2005).
- A.K. Padhi, K.S. Nanjundaswamy, and J.B. Goodenough: Phospho-olivines as positive-electrode materials for rechargeable lithium batteries. *J. Electrochem. Soc.* **144**, 1188 (1997).
- B. Lawn: *Fracture of Brittle Solids* (Cambridge University Press, New York, NY, 1993).
- A.G. Evans: Microfracture from thermal expansion anisotropy—I. Single phase systems. *Acta Metall.* **26**, 1845 (1978).
- T.C. Lu, J. Yang, Z. Suo, A.G. Evans, R. Hecht, and R. Mehrabian: Matrix cracking in intermetallic composites caused by thermal expansion mismatch. *Acta Metall. Mater.* **39**, 1883 (1991).
- J.W. Hutchinson and Z. Suo: Mixed-mode cracking in layered materials. *Adv. Appl. Mech.* **29**, 63 (1992).
- C. Ouyang, S. Shi, Z. Wang, X. Huang, and L. Chen: First-principles study of Li ion diffusion in LiFePO<sub>4</sub>. *Phys. Rev. B* **69**, 104303 (2004).
- T. Maxisch and G. Ceder: Elastic properties of olivine Li<sub>x</sub>FePO<sub>4</sub> from first principles. *Phys. Rev. B* **73**, 174112 (2006).
- K. Hsu, S. Tsay, and B. Hwang: Synthesis and characterization of nano-sized LiFePO<sub>4</sub> cathode materials prepared by a citric acid-based sol-gel route. *J. Mater. Chem.* **14**, 2690 (2004).